2013

Optimized Adaptive Control Design and NN based Trajectory Planning for a Class of Wheeled Inverted Pendulum Vehicle Models

Yang, C

http://hdl.handle.net/10026.1/1301

Trajectory Planning and Optimized Adaptive Control for a Class of Wheeled Inverted Pendulum Vehicle Models

Chenguang Yang, *Member, IEEE*, Zhijun Li, *Senior Member, IEEE*, and Jing Li

Abstract—In this paper, we investigate optimized adaptive control and trajectory generation for a class of wheeled inverted pendulum (WIP) models of vehicle systems. Aiming at shaping the controlled vehicle dynamics to be of minimized motion tracking errors as well as angular accelerations, we employ the linear quadratic regulation optimization technique to obtain an optimal reference model. Adaptive control has then been developed using variable structure method to ensure the reference model to be exactly matched in a finite-time horizon, even in the presence of various internal and external uncertainties. The minimized yaw and tilt angular accelerations help to enhance the vehicle rider's comfort. In addition, due to the underactuated mechanism of WIP, the vehicle forward velocity dynamics cannot be controlled separately from the pendulum tilt angle dynamics. Inspired by the control strategy of human drivers, who usually manipulate the tilt angle to control the forward velocity, we design a neural-network-based adaptive generator of implicit control trajectory (AGICT) of the tilt angle which indirectly "controls" the forward velocity such that it tracks the desired velocity asymptotically. The stability and optimal tracking performance have been rigorously established by theoretic analysis. In addition, simulation studies have been carried out to demonstrate the efficiency of the developed AGICT and optimized adaptive controller.

Index Terms—Linear quadratic regulation (LQR), model reference control, optimization, wheeled inverted pendulum (WIP).

I. INTRODUCTION

THE WHEELED inverted pendulum (WIP) systems have been well used in modeling of a class of modern vehicles that transport human with high safety and work capability, and therefore, it has received increasing research interest in the recent decade [21]–[23]. The simpler structure of this class of

C. Yang is with the School of Computing and Mathematics, Plymouth University, PL4 8AA Plymouth, U.K. (e-mail: chenguang.yang@plymouth.ac.uk).

Z. Li was with the Department of Automation, Shanghai Jiao Tong University, Shanghai 200240, China. He is now with the College of Automation, South China University of Technology, Guangzhou 510641, China (e-mail: zjli@ieee.org).

J. Li is with the Department of Mathematics, Xidian University, Xi'an 710071, China (e-mail: xidianjing@gmail.com).
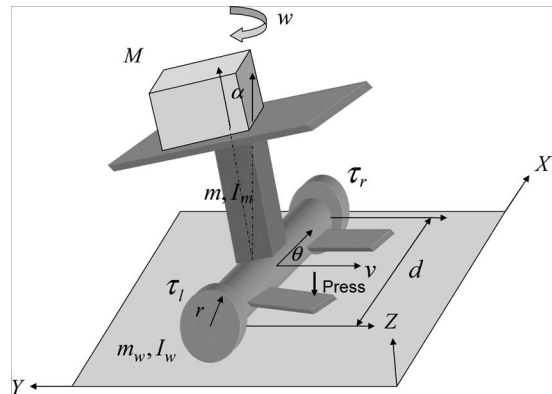
Fig. 1.　WIP model scheme.

vehicles reduces the weight of the system, and the mechanically small footprint (no caster) ensures high mobility such as quick response and high traveling ability on a bump [24], [25]. These vehicles are able to perform work that demands high power with low power and ensure high safety against overturn when unpredictable collision occurs, because the WIP controller always maintains dynamic stability. For example, the popular SEGWAY HT is able to balance a human standing on its platform while the user traverses the terrain with it.

As shown in Fig. 1, the WIP systems are different from the conventional cart and pendulum systems which have been well studied in the previous years [1]. The inverted pendulum's motion in the WIP is not planar, and the motors that drive the wheels are directly mounted on the pendulum body [24]. As the WIP systems are usually used as personal transportation vehicles moving in its terrain while balancing the pendulum, their control problem is much more challenging than controlling the cart–pendulum systems whose cart is usually constrained by a guide rail. Therefore, in the WIP control problem, it is necessary to consider the nonholonomic constraint force between the wheels and the ground which helps the mobile platform avoid the slipping or slippage. Traditionally, nonholonomic systems are subject to either only kinematic constraints which geometrically restrict the direction of mobility, e.g., wheeled mobile robot [26], [27], or only dynamic constraints due to dynamic balance at passive degrees of freedom (DOFs) where no force or torque is applied, e.g., the manipulator with passive link [28], [29]. However, the WIP systems are subject to both kinematic constraints and dynamic constraints such that the existing control designs for nonholonomic systems cannot be directly applied to the WIP systems.

In addition, the dynamics of WIP systems is governed by the underactuated configuration, i.e., the number of control inputs is less than the number of DOFs to be manipulated [2]. For WIP systems, there are only two torque inputs from motors connected to both wheels, but there are three DOFs, namely, the tilt angle of the pendulum and the forward and rotation angular velocities of the platform. Generally speaking, the underactuated systems are harder to control because many conventional methods such as computed torque control become not applicable. It should be mentioned that the analysis of the dynamics of unactuated subsystem of the underactuated system is still a challenging problem. In our previous work [30], [31], the vehicle forward velocity dynamics is regarded as zero dynamics, and zero-dynamics theories have been used to analyze the stability. As the vehicle forward velocity dynamics is directly affected by the pendulum tilt angle dynamics, in this work, we develop a new framework to manipulate the forward velocity by using the tilt angle reference trajectory as an implicit control trajectory. This is also according to the observation of a human driver's control strategy.

It is noted that a number of the existing control designs for the WIP systems are based on the idea of linearization. In addition, a feedback linearization technique has also been investigated for controlling WIP in [24], in which a two-level velocity controller was designed for position control. Although linear systems could be suitably applied to capture the nonlinear dynamics at a certain operation point, they cannot perfectly model the Lagrangian mechanical dynamics with a large operation range. Therefore, we will carry out our research using nonlinear control approach. By utilizing the unique physical property of the WIP system, we break down the overall three-DOF system into two subsystems, where the first subsystem is fully actuated while the second subsystem is unactuated. The control design of the fully actuated system is based on the model reference approach, which shapes the system dynamics to follow a reference model obtained using the linear quadratic regulation (LQR) optimization such that both the motion tracking errors and the yaw and tilt angle accelerations are minimized. We expect that it would greatly increase the rider's comfort by reducing the unnecessary acceleration while guaranteeing the tracking of the desired motion.

The underactuated subsystem of forward velocity cannot be directly controlled by the torque input but is directly affected by the tilt angle dynamics. From the observation of a human operator riding on the WIP vehicle, we see that, by properly adjusting the tilt angle, the human operator is able to well manipulate the forward velocity. This inspires us to control the forward velocity indirectly, by using the tilt angle reference trajectory, which is regarded as implicit control trajectory in this work.

It is noted that, either for control design or for trajectory planning of the WIP vehicle, a critical problem lies in the uncertainties of the system dynamics, i.e., the time-varying external disturbances and, particularly, the uncertain system parameters, for example, the rider's mass can never be known exactly beforehand. In this point of view, the development of adaptive control methods or neural network (NN)-based/fuzzy-set-based methods becomes an important issue. Adaptive con-

trol of nonlinear Lagrangian dynamic system has been extensively investigated [32]–[34]. In this work, a novel adaptive model reference control method combined with optimization technique is developed such that the dynamics of the fully actuated subsystem can exactly follow the reference model within a finite-time horizon. The proposed controller employs variable structure control method and requires little dynamics information. A novel model matching error is introduced in the controller, which is used in both controller and parameter update laws, and plays a key role in the convergence and stability analysis. On the other hand, NN and fuzzy set have been widely applied to control nonlinear dynamic systems [47]–[49], [53], nonlinear observer [50], [51], and multi-input–multioutput system [52] and have also been recently employed to deal with unknown internal interconnections and unknown time delays [4] and [8]. In [9] and [10], novel adaptive NN controllers have been developed for system with input saturation and nonlinearities. In [11], NN has been used to generate trajectory for mobile robots avoiding possible collision, while in [12], NN has been employed to control the motion tracking of mobile robots. In this work, NN will be used for approximation of the underactuated subsystem to design the adaptive generator of implicit control trajectory (AGICT). Moreover, the implicit control trajectory, namely, the reference trajectory of tilt angle, will turn back to manipulate the forward velocity.

The main contributions of this paper lie in the following: 1) A reference model for the yaw and tilt angle subsystems of the WIP system is derived using the LQR optimization approach which guarantees motion tracking and achieves the minimized angular accelerations for better riding comfort; 2) variable structure method has been employed to design the adaptive reference control in order to make the controlled dynamics to match the reference model dynamics in finite time; and 3) instead of leaving the unactuated forward velocity dynamics uncontrolled, we develop AGICT such that the reference trajectory for the tilt angle is used to indirectly affect the forward velocity to make sure that the desired velocity can be achieved. High-order NN (HONN) has been employed to construct a reference trajectory generator of the tilt angle.

The rest of this paper is organized as follows. In Section II, notations, preliminary knowledge of NN approximation, and LQR optimization are presented. In Section III, two subsystems of the underactuated WIP systems are derived with the first subsystem fully actuated while the second is unactuated. A reference trajectory generator using HONN for the tilt angle is designed in Section V such that the forward velocity is indirectly manipulated to follow its desired trajectory. In Section VI, simulation studies are carried out to verify the effectiveness of the proposed method. Concluding remarks are given in Section VII.

II. PRELIMINARIES

In this paper, we will use both the term "desired trajectory" which is predefined according to the task and the term "reference trajectory" (in Section V) which is online generated and is converging to the corresponding desired trajectory eventually. To distinguish between these two terms, we use the

subscripts "d" and "r" for the desired and reference trajectories, respectively.

Notations: The notations used in this paper, particularly those used to describe the WIP system shown in Fig. 1, are listed in the following:

x, y	the position coordinates of the midpoint of the two driving wheels;
θ	the heading angle in motion relative to the x-axis of the fixed frame;
q_v	the vector of generalized coordinates for the mobile platform with $q_v = [q_1, q_2, q_3]^{\mathrm{T}} = [\Theta, x, y]^{\mathrm{T}} \in R^3$;
α	the tilt angle relative to the z-axis of the fixed frame;
L	length of the pendulum;
M	mass of the mobile platform together with the pendulum;
m	mass of each wheel;
d	distance between the two wheels;
τ_r, τ_l	the torques of the left and right wheels;
$d_v(t), d_\alpha(t)$	the external disturbances on the mobile platform and the inverted pendulum with $d_v(t) \in R^3$ and $d_\alpha(t) \in R^1$;
I_ω, I_M	moment inertias of the wheel and mobile platform together with the pendulum;
B_v	a full-rank known input transformation matrix with $B_v \in R^{3\times2}$;
$0_{[m,n]}$	zero matrix of m rows and n columns;
$\lvert \cdot \rvert, \lVert \cdot \rVert$	vector's and matrix's L^1-norm and L^2-norm.

A. HONN Approximation

There are many well-developed approaches used to approximate an unknown function. NN is one of the most frequently employed approximation methods due to the fact that NN is shown to be capable of universally approximating any unknown continuous function to arbitrary precision [13], [37]. Similar to biological NNs, NN consists of massive simple processing units which correspond to biological neurons. With the highly parallel structure, NN is of powerful computing ability and intelligence of learning and adaptation with respect to fresh and unknown data. HONN has been shown to have strong storage capacity, approximation, and learning capability. HONN satisfies the conditions of the Stone–Weierstrass theorem and can therefore approximate any continuous function over a compact set [38], [39]. It is pointed in [40] that, by utilizing *a priori* information, HONN is very efficient in solving problems because the order or structure of HONN can be tailored to the order or structure of a given problem. The structure of HONN is expressed as follows:

$$\phi(W, \bar{z}) = W^{\mathrm{T}} S(\bar{z}), \qquad W, \ S(\bar{z}) \in R^l$$
$$S(\bar{z}) = [s_1(\bar{z}), s_2(\bar{z}), \dots, s_l(\bar{z})]^{\mathrm{T}} \qquad (1)$$
$$s_i(\bar{z}) = \prod_{j \in I_i} [s(\bar{z}_j)]^{d_j(i)}, \qquad i = 1, 2, \dots, l \qquad (2)$$

where $\bar{z} \in \Omega_{\bar{z}} \subset R^m$ is the input to HONN, l is the NN node number, $\{I_1, I_2, \dots, I_l\}$ is a collection of l not-ordered subsets of $\{1, 2, \dots, m\}$, e.g., $I_1 = \{1, 3, m\}$ and $I_2 = \{2, 4, m\}$, $d_j(i)$'s are nonnegative integers, W is an adjustable synaptic weight vector, and $s(\bar{z}_j)$ is a monotonically increasing and differentiable sigmoidal function. In this paper, it is chosen as a hyperbolic tangent function, i.e., $s(\bar{z}_j) = (e^{\bar{z}_j} - e^{-\bar{z}_j})/(e^{\bar{z}_j} + e^{-\bar{z}_j})$. For a smooth function $\varphi(\bar{z})$ over a compact set $\Omega_{\bar{z}} \subset R^m$, given a small constant real number $\mu^* > 0$, if l is sufficiently large, there exists a set of ideal bounded weights W^* such that

$$\max |\varphi(\bar{z}) - \phi(W^*, \bar{z})| < \mu(\bar{z}), \qquad |\mu(\bar{z})| < \mu^*. \qquad (3)$$

From the universal approximation results for NNs [41], it is known that the constant μ^* can be made arbitrarily small by increasing the NN node number l.

Lemma 1 [42]: Consider the basis functions of HONN (1) with $\bar{z}$ being the input vector. The following properties of HONN will be used in the proof of closed-loop system stability:

$$\lambda_{\max} \left[S(\bar{z}) S^{\mathrm{T}}(\bar{z}) \right] < 1, \qquad S^{\mathrm{T}}(\bar{z}) S(\bar{z}) < l \qquad (4)$$

where $\lambda_{\max}(M)$ denotes the maximum eigenvalue of M.

Lemma 2 [43]: Consider a C^r function $f : R^{k+n} \to R^n$ with $f(a, b) = 0_{[n,1]}$ and $\mathrm{rank}(Df(a,b)) = n$, where $Df(a, b) = (\partial f(x, y)/\partial y)|_{(x,y)=(a,b)} \in R^{n\times n}$. Then, there exist a neighborhood A of a in R^k and a unique C^r function $g : A \to R^n$ such that $g(a) = b$ and $f(x, g(x)) = 0_{[n,1]} \ \forall x \in A$.

B. Finite-Time Linear Quadratic Regulator

Given a linear system with completely stabilizable pair $[A, B]$ [44]

$$\dot{x} = Ax + Bu \quad x(t_0) = x_0, \qquad x \in R^n; \quad u \in R^n \qquad (5)$$

the optimal control $u^*(t)$, $T > 0$, that minimizes the following performance index:

$$J = \int_{t_0}^{t_f} \left((x - x_d)^{\mathrm{T}} Q (x - x_d) + u^{\mathrm{T}} R u \right) dt,$$
$$R = R^{\mathrm{T}} > 0; \quad Q = Q^{\mathrm{T}} > 0 \qquad (6)$$

is given by

$$au^* = -R^{-1} B^{\mathrm{T}} (Px + s) \qquad (7)$$

with P as the solution of the following Riccati equation:

$$-\dot{P} = PA + A^{\mathrm{T}} P - PBR^{-1} B^{\mathrm{T}} P + Q \quad P(t_f) = 0_{[n,n]} \qquad (8)$$

and s as the solution of

$$-\dot{s} = (A - BR^{-1} B^{\mathrm{T}} P)^{\mathrm{T}} s + Q x_d \quad s(t_f) = 0_{[n,1]}. \qquad (9)$$

III. DYNAMICS OF MOBILE WIPs

The dynamics model of mobile WIPs studied in this work is described by the following Lagrangian formulation:

$$\begin{bmatrix} D_v & D_{v\alpha} \\ D_{\alpha v} & D_\alpha \end{bmatrix} \begin{bmatrix} \ddot{q}_v \\ \ddot{\alpha} \end{bmatrix} + \begin{bmatrix} C_v & C_{v\alpha} \\ C_{\alpha v} & C_\alpha \end{bmatrix} \begin{bmatrix} \dot{q}_v \\ \dot{\alpha} \end{bmatrix}$$
$$+ \begin{bmatrix} F_v \\ F_\alpha \end{bmatrix} + \begin{bmatrix} G_v \\ G_\alpha \end{bmatrix} + \begin{bmatrix} d_v \\ d_\alpha \end{bmatrix} = \begin{bmatrix} B_v \tau_v \\ 0 \end{bmatrix} + \begin{bmatrix} J_v^{\mathrm{T}} \lambda \\ 0 \end{bmatrix} \qquad (10)$$

where $\tau_v = [\tau_l, \tau_r]$ represents the torques produced by the two wheel motors and B_v is a known matrix. In this work, we do not consider any constraints on the input torques, but some recent development on adaptive control with input constraints [9], [10] can be applied in our model. The term J_v is the matrix related to nonholonomic constraints of the mobile platform of WIP defined as

$$J_v = [0, \sin\theta, -\cos\theta] \tag{11}$$

and the nonholonomic constraints are described as

$$J_v \dot{q}_v = 0. \tag{12}$$

It is always possible to find a set of smooth and linearly independent vector fields $\Phi_1(q)$ and $\Phi_2(q)$ constituting the matrix $\Phi = [\Phi_1(q), \Phi_2(q)] \in R^{3\times 2}$ with full rank $\Phi^T\Phi$, which, in the local coordinates, satisfy the following relation:

$$\Phi^T J_v^T = 0_{[2,1]}. \tag{13}$$

Constraint equation (12) implies the existence of vector $\dot{\chi} = [\omega, v]^T \in R^2$ with ω representing the component of the angular velocity of the platform denoted in Fig. 1 and v representing the forward velocity of the mobile platform such that

$$\dot{q}_v = \Phi(q)\dot{\chi}. \tag{14}$$

Let us define new variables

$$\dot{\zeta} = [\dot{\chi}, \dot{\alpha}]^T = [\dot{\zeta}_1, \dot{\zeta}_2, \dot{\zeta}_3]^T = [\omega, v, \dot{\alpha}]^T \tag{15}$$

and multiply $\mathrm{diag}[\Phi^T, I]$ by both sides of (10) to eliminate J_v^T; the dynamics of WIP can be expressed as

$$D(\zeta)\ddot{\zeta} + C(\zeta, \dot{\zeta})\dot{\zeta} + G(\zeta) + f_d = \tau \tag{16}$$

where

$$D(\zeta) = \begin{bmatrix} \Phi^T D_v \Phi & \Phi^T D_{v\alpha} \\ D_{\alpha v} \Phi & D_\alpha \end{bmatrix}$$
$$= \begin{bmatrix} d_{11} & 0 & 0 \\ 0 & d_{22} & d_{23} \\ 0 & d_{32} & d_{33} \end{bmatrix}$$
$$C(\zeta, \dot{\zeta}) = \begin{bmatrix} \Phi^T D_v \dot{\Phi} + \Phi^T C_v \Phi & \Phi^T C_{v\alpha} \\ D_{\alpha v} \dot{\Phi} + C_{\alpha v} \Phi & C_\alpha \end{bmatrix}$$
$$= \begin{bmatrix} c_{11} & 0 & c_{13} \\ 0 & 0 & c_{23} \\ c_{31} & 0 & 0 \end{bmatrix}$$
$$f_d = \begin{bmatrix} \Phi^T d_v \\ d_\alpha \end{bmatrix} = \begin{bmatrix} \bar{d}_1 \\ \bar{d}_2 \\ \bar{d}_3 \end{bmatrix}$$
$$G(\zeta) = \begin{bmatrix} \Phi^T G_v \\ G_\alpha \end{bmatrix} = \begin{bmatrix} 0 \\ 0 \\ g_3 \end{bmatrix}$$
$$\tau = \begin{bmatrix} \Phi^T B_v \tau_v \\ 0 \end{bmatrix} = \begin{bmatrix} \tau_1 \\ \tau_2 \\ 0 \end{bmatrix} \tag{17}$$

with $d_{11} = d^2 m/2 + I_M d^2/2R^2 + I_\omega + ML^2 \sin^2\alpha$, $d_{22} = 2m + 2I_M/R^2 + M$, $d_{33} = ML^2 + I_M$, and $d_{23} = d_{32} = ML\cos\alpha$; $c_{11} = (1/2)ML^2\dot{\alpha}\sin 2\alpha$, $c_{13} = (1/2)\omega ML^2 \sin 2\alpha$, $c_{23} = -ML\dot{\alpha}\sin\alpha$, and $c_{31} = -(1/2)\omega ML^2\sin 2\alpha$; and $g_3 = -MgL\sin\alpha$.

Remark 1: It should be mentioned that, due to the unknown system parameters in the aforementioned dynamics formulation, the dynamics matrices are actually unknown for control design.

The following two properties are well known for the Lagrange–Euler formulation of robotic dynamics.

Property 1: The matrix $D(\zeta)$ is symmetric and positive definite.

Property 2: The matrix $2C(\zeta, \dot{\zeta}) - \dot{D}(\zeta)$ is a skew-symmetric matrix.

Expanding (16), we obtain three equations in which the first one can be regarded as ζ_1 subsystem described as follows:

$$\Sigma_{\zeta_1} : d_{11}\ddot{\zeta}_1 + c_{11}\dot{\zeta}_1 + c_{13}\dot{\zeta}_3 + \bar{d}_1 = \tau_1. \tag{18}$$

The second and the third equations are

$$d_{22}\ddot{\zeta}_2 + d_{23}\ddot{\zeta}_3 + c_{23}\dot{\zeta}_3 + \bar{d}_2 = \tau_2$$
$$d_{32}\ddot{\zeta}_2 + d_{33}\ddot{\zeta}_3 + c_{31}\dot{\zeta}_1 + \bar{d}_3 + g_3 = 0 \tag{19}$$

from which we could clearly see the underactuated configuration, i.e., it is not possible to control ζ_2 and ζ_3 independently.

By substituting the third equation into the second one, we obtain the ζ_2 subsystem and ζ_3 subsystem as follows:

$$\Sigma_{\zeta_2} : \frac{d_{22}d_{33} - d_{23}^2}{d_{33}}\ddot{\zeta}_2 - \frac{d_{23}}{d_{33}}(c_{31}\dot{\zeta}_1 + g_3 + \bar{d}_3(\dot{\zeta}_3))$$
$$+ c_{23}\dot{\zeta}_3 + \bar{d}_2 = \tau_2 \tag{20}$$
$$\Sigma_{\zeta_3} : \frac{d_{22}d_{33} - d_{23}^2}{d_{23}}\ddot{\zeta}_3 + \frac{d_{22}}{d_{23}}(c_{31}\dot{\zeta}_1 + g_3 + \bar{d}_3)$$
$$- c_{23}\dot{\zeta}_3 - \bar{d}_2 = -\tau_2. \tag{21}$$

Remark 2: Note that an implicit assumption that the pendulum tilt angle $\zeta_3 = \alpha \in (-(\pi/2), \pi/2)$ such that $d_{23} \neq 0$ is made to derive (21). This assumption is very reasonable as the dynamics when the tilt angle is beyond $-(\pi/2)$ or $\pi/2$ is out of the research interest.

IV. CONTROL OF ζ_1 AND ζ_3 SUBSYSTEMS

A. Subsystem Dynamics

For convenience, let us combine the dynamics of subsystems Σ_{ζ_1} and Σ_{ζ_3} as follows:

$$\mathcal{M}\ddot{\xi} + \mathcal{C}\dot{\xi} + h = \tau \tag{22}$$

where

$$\mathcal{M} = \begin{bmatrix} d_{11} & 0 \\ 0 & \frac{d_{22}d_{33} - d_{23}^2}{d_{23}} \end{bmatrix}$$
$$\mathcal{C} = \begin{bmatrix} c_{11} & c_{13} \\ c_{31} & \frac{1}{2}\frac{d}{dt}\frac{d_{22}d_{33} - d_{23}^2}{d_{23}} \end{bmatrix}$$
$$h = \begin{bmatrix} \bar{d}_1 \\ \frac{d_{22}}{d_{23}}(g_3 + \bar{d}_3) - \bar{d}_2 \end{bmatrix}$$
$$+ \begin{bmatrix} 0 & 0 \\ \frac{d_{22} - d_{23}}{d_{23}}c_{31} & -c_{23} - \frac{1}{2}\frac{d}{dt}\frac{d_{22}d_{33} - d_{23}^2}{d_{23}} \end{bmatrix} \begin{bmatrix} \dot{\xi}_1 \\ \dot{\xi}_2 \end{bmatrix}$$
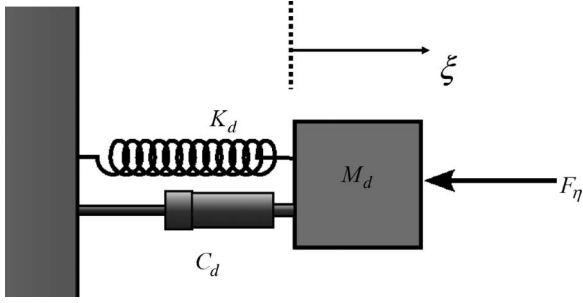$$\tau = [\tau_1 \quad -\tau_2]^T \quad \xi = [\zeta_1 \quad \zeta_3]^T.$$

Fig. 2. Mass–spring–damper impedance model.

Recall that the inertia matrix $D(\zeta)$ is positive definite and symmetric, so we know that the terms d_{11} and $d_{22}d_{33} - d_{23}^2$ are positive. Furthermore, according to Remark 2, we know that $(d_{22}d_{33} - d_{23}^2)/d_{23}$ is also positive. In addition, due to the fact that $\dot{D} - 2C$ is skew-symmetric, we have the following properties.

Property 3 [45]: The inertia matrix $\mathcal{M}$ is positive definite and symmetric.

Property 4 [45]: The matrix $\dot{\mathcal{M}} - 2\mathcal{C}$ is skew-symmetric such that $x^{\mathrm{T}}(\dot{\mathcal{M}} - 2\mathcal{C})x = 0 \; \forall x \in R^2$.

In addition, it is well known in the robotics literature that the following property holds.

Property 5 [45]: There exist unknown positive scalars θ_M, θ_C, θ_{h1}, and θ_{h2} such that $\|\mathcal{M}(\xi)\| \leq \theta_M$, $\|\mathcal{C}\| \leq \theta_C \|\dot{\xi}\|$, and $\|h\| \leq \theta_{h1}\|\xi\|\|\dot{\xi}\| + \theta_{h2}$.

B. Optimal Reference Model

To design the model reference control of subsystem dynamics (22), we need to construct a reference model for the ζ_1 and ζ_3 subsystems. We consider an *impedance model* with *virtual force* as follows:

$$M_r\ddot{\xi} + C_r\dot{\xi} + K_r\xi = -F_\eta(\xi_d, \dot{\xi}_d) \tag{23}$$

where M_r, C_r, and K_r are the desired inertia, damping, and stiffness matrices, respectively, and F_η can be regarded as a *virtual force*. This reference model can be illustrated by a mass–spring–damper system shown in Fig. 2, where the virtual force F_η is a term introduced to drive the position ξ and velocity $\dot{\xi}$ of the mass to track the desired position ξ_d and desired velocity $\dot{\xi}_d$. It should be emphasized that this force term F_η only exists virtually but not physically. As the control objective is to make the closed-loop dynamics of the controlled subsystem (22) match the dynamics of the reference model (23), we should suitably choose the parameters of the reference model such that it not only guarantees the motion tracking but also takes care of the rider's comfort, e.g., it must be overdamped to guarantee no overshooting and no oscillation. The virtual impedance model provides a kind of cushion effect for better riding experience, and when there is no artificial force F_η (e.g., the rider lets go the wheel and pedal), the yaw and tilt angles ζ_1 and ζ_3 will tend to rest on the zero position.

In order to choose the optimal values of the reference model parameters, we introduce the following performance index:

$$I_P = \int_{t_0}^{t_f} (e^{\mathrm{T}}Qe + \ddot{\xi}^{\mathrm{T}}M_d\ddot{\xi})\, dt \tag{24}$$

which minimizes both the motion tracking error

$$e = \xi - \xi_d \tag{25}$$

and the yaw and tilt angular accelerations. From (24), we see that the performance index minimizes both the tracking error and angular accelerations. From the rider's experience, we know that, the less the angular acceleration is, the better the feeling is, so we aim to enhance the rider's comfort by reducing any unnecessary angular accelerations and to reduce the torques that wheel motors produce, while ensuring motion tracking performance. Now, let us consider how to minimize the performance index I_P by suitably designing C_d, K_r, and F_η. In order to apply the LQR optimization technique, we rewrite the reference model (23) as

$$\dot{\bar{\xi}} = A\bar{\xi} + Bu \tag{26}$$

with

$$\bar{\xi} = [\xi^{\mathrm{T}}, \dot{\xi}^{\mathrm{T}}]^{\mathrm{T}} \quad \bar{\xi}_d = \left[\xi_d^{\mathrm{T}}, \dot{\xi}_d^{\mathrm{T}}\right]^{\mathrm{T}} \quad Q = \begin{bmatrix} q_1 & 0 \\ 0 & q_2 \end{bmatrix} \tag{27}$$

$$A = \begin{bmatrix} 0_{[2,2]} & I_{[2,2]} \\ 0_{[2,2]} & 0_{[2,2]} \end{bmatrix} \quad B = \left[0_{[2,2]}, I_{[2,2]}\right]^{\mathrm{T}} \tag{28}$$

$$u = -M_d^{-1}[K_r, C_d]\bar{\xi} - M_d^{-1}F_\eta(\xi_d, \dot{\xi}_d). \tag{29}$$

Noting that $u = \ddot{\xi}$ and introducing $\bar{Q}$ defined as

$$\bar{Q} = \begin{bmatrix} Q & 0_{[2,2]} \\ 0_{[2,2]} & 0_{[2,2]} \end{bmatrix} \tag{30}$$

we can then rewrite the performance index (24) as

$$P_{\bar{I}} = \int_{t_0}^{t_f} \left((\bar{\xi} - \bar{\xi}_d)^{\mathrm{T}}\bar{Q}(\bar{\xi} - \bar{\xi}_d) + u^{\mathrm{T}}M_d u\right) dt. \tag{31}$$

If we regard u as the control input to system (26), then the minimization of (31) subject to dynamics constraint (26) becomes a typical LQR control design problem. According to the LQR optimal control technique reviewed in Section II-C, the solution of u that minimizes (31) is

$$u = -M_d^{-1}B^{\mathrm{T}}P\bar{\xi} - M_r^{-1}B^{\mathrm{T}}s \tag{32}$$

where P is the solution of the following differential equation:

$$-\dot{P} = PA + A^{\mathrm{T}}P - PBM_d^{-1}B^{\mathrm{T}}P + \bar{Q} \quad P(t_f) = 0_{[4,4]} \tag{33}$$

and s is the solution of the following differential equation:

$$-\dot{s} = \left(A - BM_d^{-1}B^{\mathrm{T}}P\right)^{\mathrm{T}}g + \bar{Q}\bar{\xi}_d \quad s(t_f) = 0_{[4,1]}. \tag{34}$$

Comparing (29) and (32), we can see that the matrices K_r and C_d can be calculated in the following manner:

$$[K_r, C_d] = B^{\mathrm{T}}P \quad F_\eta = B^{\mathrm{T}}s. \tag{35}$$

Remark 3: To obtain a reference model with minimizing (24), we first need to choose values of q_1 and q_2 for the weighting matrix Q as well as the desired mass M_r; then, we can calculate K_r and C_d according to (33)–(35).

Remark 4: It should be emphasized that the performance index (31) is a finite-time integration such that, when the minimization of (31) is achieved using (32), we always have $e = 0_{[2,1]} \ \forall t > t_f$.

C. Model Matching Errors

By using $e = \xi - \xi_d$, the reference model (23) can be rewritten as

$$M_r\ddot{e} + C_r\dot{e} + K_r e = -\eta \tag{36}$$

with

$$\eta = F_\eta + M_r\ddot{\xi}_d + C_r\dot{\xi}_d + K_r\xi_d. \tag{37}$$

We can see that the objective of the control design becomes to look for a proper control input torque τ in (22) such that the dynamics (22) match the desired reference model dynamics (36). In order to measure the difference between the subsystem dynamics (22) and the reference model dynamics (36), we introduce the following matching error defined as:

$$w = M_r\ddot{e} + C_r\dot{e} + K_r e + \eta \tag{38}$$

such that, when the following condition is achieved:

$$w(t) = 0_{[2,1]}, \qquad t > t_f \tag{39}$$

the subsystem dynamics (22) would exactly match the desired reference model dynamics (36).

For convenience of the following analysis, we define an augmented matching error as

$$\bar{w} = K_\eta w = \ddot{e} + C_m\dot{e} + K_m e + K_\eta\eta \tag{40}$$

where $C_m = M_r^{-1}C_r$, $K_m = M_r^{-1}K_r$, and $K_\eta = M_d^{-1}$.

Remark 5: The virtual mass matrix M_r is always chosen to be positive definite such that it is invertible and $\bar{w}$ in (40) is well defined.

By choosing two positive definite matrices Λ and Γ such that $\Lambda + \Gamma = C_m$ and $\Gamma\Lambda + \dot{\Lambda} = K_m$, we could further rewrite the augmented matching error $\bar{w}$ as

$$\bar{w} = \ddot{e} + (\Lambda + \Gamma)\dot{e} + (\Gamma\Lambda + \dot{\Lambda})e + \dot{\eta}_l + \Gamma\eta_l \tag{41}$$

where η_l satisfies

$$\dot{\eta}_l + \Gamma\eta_l = K_\eta\eta. \tag{42}$$

By defining a filtered matching error

$$z = \dot{e} + \Lambda e + \eta_l \tag{43}$$

we see that the augmented matching error $\bar{w}$ can be written as

$$\bar{w} = \dot{z} + \Gamma z \tag{44}$$

which implies that z could be obtained by passing $\bar{w}$ through a filter. From (44) and (40), we see that $z = 0_{[2,1]}$ and, subsequently, $\dot{z} = 0_{[2,1]}$ will lead to $w = 0_{[2,1]}$, i.e., matching error diminished. Then, the yaw and tilt angle subsystem dynamics (22) would exactly match the reference model (23). According to Remark 4, after a finite time t_f, we will have $\xi = \xi_d$. In the next section, we will design an adaptive controller which guarantees that there exists a finite time $t_z \ll t_f$ such that $z = 0_{[2,1]}$ for $t > t_z$.

D. Adaptive Control Design

1) Controller Structure: In this section, we are ready to discuss the details of the adaptive control design. We propose the control input of the subsystem (22) as

$$\tau = \tau_{\mathrm{ct}} + \tau_{\mathrm{fb}} \tag{45}$$

where τ_{ct} and τ_{fb} are the computed torque control input and the feedback torque control input, respectively. The feedback torque control input is given by

$$\tau_{\mathrm{fb}} = -K\,\mathrm{sgn}(z) \tag{46}$$

where K is a diagonal positive definite matrix with $k_{\min}$ denoting the minimal element on the diagonal and $\mathrm{sgn}(\cdot)$ is the sign function.

The computed torque control input is designed as

$$\tau_{\mathrm{ct}} = -Y(\ddot{\xi}_r, \dot{\xi}_r, z)\hat{\Theta} \tag{47}$$

where the trajectories ξ_r and $\dot{\xi}_r$ are defined as follows:

$$\dot{\xi}_r = \dot{\xi}_d - \Lambda e - \eta_l$$
$$\ddot{\xi}_r = \ddot{\xi}_d - \Lambda\dot{e} - \dot{\eta}_l \tag{48}$$

and $\hat{\Theta}$ is the estimate of $\Theta = [\theta_D, \theta_C, \theta_{h1}, \theta_{h2}]^{\mathrm{T}}$ (refer to Property 5) and

$$Y(\ddot{\xi}_r, \dot{\xi}_r, z)$$
$$= \begin{bmatrix} \|\ddot{\xi}_r\|\mathrm{sgn}(z_1) & \|\dot{\xi}\|\|\dot{\xi}_r\|\mathrm{sgn}(z_1) & \|\dot{\xi}\|\|\xi\|\mathrm{sgn}(z_1) & \mathrm{sgn}(z_1) \\ \|\ddot{\xi}_r\|\mathrm{sgn}(z_2) & \|\dot{\xi}\|\|\dot{\xi}_r\|\mathrm{sgn}(z_2) & \|\dot{\xi}\|\|\xi\|\mathrm{sgn}(z_2) & \mathrm{sgn}(z_2) \end{bmatrix}. \tag{49}$$

In the following, for convenience, we use Y instead of $Y(\ddot{\xi}_r, \dot{\xi}_r, z)$, where it does not result in any confusion.

Remark 6: The potential drawback caused by the $\mathrm{sgn}(\cdot)$ function used in (46) and (49), such as chattering problems, can be avoided by replacing $\mathrm{sgn}(\cdot)$ with hyperbolic tangent function $\tanh(\cdot)$ or saturation function $\mathrm{sat}(\cdot)$ [46]. For convenience of our analysis, we keep using $\mathrm{sgn}(\cdot)$ in the following theoretic analysis. It is trivial but tedious to use $\tanh(\cdot)$ or $\mathrm{sat}(\cdot)$ for theoretic analysis.

To obtain $\hat{\Theta}$, we develop the following parameter update law:

$$\dot{\hat{\Theta}} = \Gamma_{\Theta}^{-1} Y^{\mathrm{T}} z \tag{50}$$

where Γ_{Θ} is a diagonal positive definite matrix.

2) Control Performance Analysis:

Lemma 3: Consider the closed-loop control system consisting of the yaw and tilt angle subsystem (22) and the controller (45). The following results hold: 1) All the signals in the closed loop are uniformly bounded, and 2) the filtered matching error z will converge to zero, i.e., $\lim_{t \to 0} z = 0_{[2,1]}$.

Proof: To prove the aforementioned lemma, let us consider the following Lyapunov-like composite energy function:

$$V_1(t) = U_1(t) + U_2(t) \tag{51}$$

where

$$U_1(t) = \frac{1}{2} z^{\mathrm{T}} \mathcal{M}(\xi) z \quad U_2(t) = \frac{1}{2} \tilde{\Theta}^{\mathrm{T}}(t) \Gamma_{\Theta}^{\mathrm{T}} \tilde{\Theta}(t) \tag{52}$$

with $\tilde{\Theta}(t) = \Theta(t) - \hat{\Theta}(t)$.

According to Property 5 and the definitions of Y in (49), we have

$$- z^{\mathrm{T}} \left(\mathcal{M}(\xi) \ddot{\xi}_r + \mathcal{C}(\xi, \dot{\xi}) \dot{\xi}_r + h(\xi, \dot{\xi}) \right)$$

$$\leq \|z\| \left(\left\| \mathcal{M}(\xi) \ddot{\xi}_r \right\| + \left\| \mathcal{C}(\xi, \dot{\xi}) \dot{\xi}_r \right\| + \left\| h(\xi, \dot{\xi}) \right\| \right)$$

$$\leq \|z\| \left(\|\mathcal{M}(\xi)\| \|\ddot{\xi}_r\| + \left\| \mathcal{C}(\xi, \dot{\xi}) \right\| \|\dot{\xi}_r\| + \left\| h(\xi, \dot{\xi}) \right\| \right)$$

$$\leq \|z\| \left(\theta_M \|\ddot{\xi}_r\| + \theta_C \|\dot{\xi}\| \|\dot{\xi}_r\| + \theta_{h1} \|\xi\| \|\dot{\xi}\| + \theta_{h2} \right)$$

$$= z^{\mathrm{T}} \mathrm{sgn}(z) \left(\theta_M \|\ddot{\xi}_r\| + \theta_C \|\dot{\xi}\| \|\dot{\xi}_r\| + \theta_{h1} \|\xi\| \|\dot{\xi}\| + \theta_{h2} \right)$$

$$= z^{\mathrm{T}} Y \Theta. \tag{53}$$

Then, by considering the closed-loop dynamics (43) and the controller (45), we obtain

$$\dot{U}_1 = z^{\mathrm{T}} \mathcal{M}(\xi) \dot{z} + \frac{1}{2} z^{\mathrm{T}} \dot{\mathcal{M}}(\xi) z$$

$$= z^{\mathrm{T}} \mathcal{M}(\xi) \dot{z} + z^{\mathrm{T}} \mathcal{C}(\xi, \dot{\xi}) z$$

$$= z^{\mathrm{T}} \left(-\mathcal{M}(\xi) \ddot{\xi}_r - \mathcal{C}(\xi, \dot{\xi}) \dot{\xi}_r - h(\xi, \dot{\xi}) + u \right)$$

$$\leq z^{\mathrm{T}} \left(Y \Theta - Y \hat{\Theta} - K \, \mathrm{sgn}(z) \right)$$

$$= z^{\mathrm{T}} \left(Y \tilde{\Theta} - K \, \mathrm{sgn}(z) \right) \tag{54}$$

where we have used Property 4 in the second equality.

On the other hand, we have

$$\dot{U}_2 = -\dot{\hat{\Theta}}^{\mathrm{T}} \Gamma_{\Theta}^{\mathrm{T}} \tilde{\Theta} = -z^{\mathrm{T}} Y \tilde{\Theta}. \tag{55}$$

According to (51), (54), and (55), we obtain the boundedness of $V_1(t)$ according to the following derivation:

$$\dot{V}_1 = \dot{U}_1 + \dot{U}_2 \leq -z^{\mathrm{T}} K \, \mathrm{sgn}(z) \leq 0. \tag{56}$$

This implies that both U_1 and U_2 are bounded, and consequently, z and $\tilde{\Theta}$ are bounded. Integrating both sides of (56) and noting the fact that

$$- z^{\mathrm{T}} K \, \mathrm{sgn}(z) = -K|z| \leq -\|K\| \|z\| \leq -k_{\min} \|z\| \leq 0 \tag{57}$$

we see that

$$\int_0^{\infty} k_{\min} \|z\| \, dt \leq V_1(0) \tag{58}$$

from which one can immediately obtain $\lim_{t \to 0} \|z\| = 0$, which is equivalent to $\lim_{t \to 0} z = 0_{[2,1]}$. This completes the proof. ∎

Theorem 1: There exists a finite time t_z such that $z = 0_{[2,1]}$ for $t > t_z \ll t_f$.

Proof: This proof uses a contradiction argument. Assume that $\|z\| > 0$ for $t > 0$.

There exist two constants $\bar{m}_{\min}$ and $\bar{m}_{\max}$ such that $\bar{m}_{\min} \leq \|\mathcal{M}\| \leq \bar{m}_{\max}$, and consequently, the following inequalities can be obtained from (52)

$$\frac{1}{2} \bar{m}_{\min} \|z\|^2 \leq U_1 \leq \frac{1}{2} \bar{m}_{\max} \|z\|^2. \tag{59}$$

At the same time, we also have that

$$\frac{d}{dt} \frac{U_1}{\|z\|} = \frac{\dot{U}_1}{\|z\|} - \frac{U_1}{\|z\|^2} \frac{d\|z\|}{dt}. \tag{60}$$

Integrating both sides of the aforementioned equation, we arrive at

$$\int_0^t \frac{\dot{U}_1}{\|z\|} \, dt = \frac{U_1}{\|z\|} \bigg|_0^t + \int_0^t \frac{U_1}{\|z\|^2} \, d\|z\|. \tag{61}$$

Combining the aforementioned equation with (59), we have

$$\bar{m}_{\min} \|z\| - \bar{m}_{\min} \|z(0)\| \leq \int_0^t \frac{\dot{U}_1}{\|z\|} \, dt$$
$$\leq \bar{m}_{\max} \|z\| - \bar{m}_{\max} \|z(0)\|. \tag{62}$$

Recalling the boundedness of $\|z\|$ and the fact that $\lim_{t \to 0} \|z\| = 0$, we obtain the boundedness of $\int_0^{\infty} (\dot{U}_1 / \|z\|) dt$, which implies that

$$\lim_{t \to \infty} \frac{\dot{U}_1}{\|z\|} = 0. \tag{63}$$

On the other hand, according to (54) and (58), we can prove that

$$\dot{U}_1 \leq - \left(k_{\min} - \|Y\| \|\tilde{\Theta}\| \right) \|z\|. \tag{64}$$

In addition, if $k_{\min}$ is sufficiently large, then there exists a constant k' such that $k' = k_{\min} - \|Y\| \|\tilde{\Theta}\| > 0$. If $\|z\| > 0$ $\forall t > 0$, then we would have $\dot{U}_1 / \|z\| \leq -k' < 0$. This obviously conflicts with (63), such that we see that there must exist a finite t_z such that $z = 0_{[2,1]}$ for $t > t_z$. Further analysis shows that, the larger the $k_{\min}$ chosen, the smaller the t_z will be. Therefore, we could always be able to properly choose t_f and $k_{\min}$ to guarantee that $t_z \ll t_f$. This completes the proof. ∎

V. AGICT FOR ζ_2 SUBSYSTEM

According to the observation of WIP vehicle riders, it can be concluded that human riders are usually able to adjust the tilt angle suitable to maintain the forward velocity at a desired value. However, until now, to our best knowledge, there has been very less study to discuss the automatic control of the forward velocity for the underactuated WIP vehicles. In this work, we attempt to set up a framework to design an AGICT such that the tilt angle reference trajectory can be used to manipulate the forward velocity to track the desired trajectory. As previously discussed, after finite time, ζ_1 and ζ_3 will exactly track ζ_{1d} and ζ_{3d}, such that the forward velocity dynamics in the second equation of (19) becomes a double integrator system as follows:

$$
\ddot{\zeta}_2 = -\frac{1}{ML\cos\zeta_{3d}}(ML^2 + I_M)\ddot{\zeta}_{3d} + \frac{1}{ML\cos\zeta_{3d}}
$$
$$
\times \left(\frac{1}{2}\dot{\zeta}_{1d}ML^2\sin 2\zeta_{3d} + MgL\sin\zeta_{3d} - \bar{d}_3\right). \quad (65)
$$

Let $\varphi = [\varphi_1, \varphi_2] = [\zeta_2, \dot{\zeta}_2]$, $\phi = [\phi_1, \phi_2] = [\zeta_{3d}, \dot{\zeta}_{3d}]$, and $v = \ddot{\zeta}_{3d}$. Then, (65) can be rewritten as

$$
\dot{\varphi}_1 = \varphi_2
$$
$$
\dot{\varphi}_2 = f(\varphi, \phi, v) \quad (66)
$$

with

$$
f(\varphi, \phi, v) = b(\phi_1)v + \frac{1}{ML\cos\phi_1}
$$
$$
\times \left(\frac{1}{2}\dot{\omega}_d ML^2\sin 2\phi_1 + MgL\sin\phi_1 - \bar{d}_3\right) (67)
$$

$$
b(\phi_1) = -\frac{1}{ML\cos\phi_1}(ML^2 + I_M) \quad (68)
$$

$$
\dot{\phi}_1 = \phi_2
$$
$$
\dot{\phi}_2 = v. \quad (69)
$$

Remark 7: Considering Remark 2, we can see that $\partial f(\varphi, \phi, v)/\partial v = b(\phi_1) < 0$.

Consider the desired forward position and forward velocity of the vehicle as ζ_{2d} and $\dot{\zeta}_{2d}$, respectively. Then, our design objective is to construct a v (subsequently, ϕ_1 and ϕ_2) such that φ_1 and φ_2 of system (66) follow φ_{1r} and φ_{2r} generated from the following reference model:

$$
\dot{\varphi}_{1r} = \varphi_{2r}
$$
$$
\dot{\varphi}_{2r} = f_d(\zeta_{2d}, \dot{\zeta}_{2d}, \varphi_r) \quad (70)
$$

where $\varphi_r = [\varphi_{1r}, \varphi_{2r}]$ and $f_d(\zeta_{2d}, \dot{\zeta}_{2d}, \varphi_r) = -k_1(\varphi_{1r} - \zeta_{2d}) - k_2(\varphi_{2r} - \dot{\zeta}_{2d}) + \ddot{\zeta}_{2d}$. It can be easily checked that reference model (70) ensures that $\varphi_{1r} \to \zeta_{2d}$ and $\varphi_{2r} \to \dot{\zeta}_{2d}$, with positive k_1 and k_2 to be specified by the designer. It should be mentioned that optimization has also been widely applied in robotic trajectory planning [54], and the LQR-based optimization method used in Section IV-B can also be used here to

choose optimal values for k_1 and k_2, but for simplicity, we omit further discussion here. According to implicit function theorem (refer to Lemma 2)-based NN design [55], there must exist a function f_v

$$
v^* = f_v(\zeta_{2d}, \dot{\zeta}_{2d}, \varphi, \phi) \quad (71)
$$

such that

$$
f(\varphi, \phi, v^*) = f_d(\zeta_{2d}, \dot{\zeta}_{2d}, \varphi). \quad (72)
$$

Referring to Section II-B, we can see that there exists an ideal HONN weight such that

$$
v^* = W^{*T}S(z) + \epsilon, \qquad z = [\zeta_{2d}, \dot{\zeta}_{2d}, \varphi, \phi]^T \quad (73)
$$

where ϵ is the NN approximation error. Let us employ a HONN to approximate v^* as follows:

$$
\hat{v} = \hat{W}^T(k)S(z). \quad (74)
$$

Substituting $\hat{v}$ into (66) and using $f(\phi, \varphi, v^*) = f_d(\zeta_{2d}, \dot{\zeta}_{2d}, \phi)$, we have

$$
\dot{\varphi}_1 = \varphi_2
$$
$$
\dot{\varphi}_2 = f_d(\zeta_{2d}, \dot{\zeta}_{2d}, \phi) + b(v')\left(\tilde{W}^T S(z) - \epsilon\right) \quad (75)
$$

where mean value theorem is used to obtain $f(\phi, \varphi, \hat{v}) - f(\phi, \varphi, v^*) = b(v')(\hat{v} - v^*) = b(v')(\tilde{W}^T S(z) - \epsilon)$, where $\tilde{W} = \hat{W} - W^*$ and $v' \in [\min\{v^*, \hat{v}\}, \max\{v^*, \hat{v}\}]$.

Define $\tilde{\varphi}_1 = \varphi_1 - \varphi_{1r}$ and $\tilde{\varphi}_2 = \varphi_2 - \varphi_{2r}$ such that $\tilde{\varphi} = \hat{\varphi} - \varphi$. Then, the comparison between (70) and (75) yields

$$
\dot{\tilde{\varphi}}_1 = \tilde{\varphi}_2
$$
$$
\dot{\tilde{\varphi}}_2 = f_d(\zeta_{2d}, \dot{\zeta}_{2d}, \phi) - f_d(\zeta_{2d}, \dot{\zeta}_{2d}, \phi_d)
$$
$$
+ b(v')\left(\tilde{W}^T S(z) - \epsilon\right)
$$
$$
= -k_1\tilde{\varphi}_1 - k_2\tilde{\varphi}_2 + b(v')\left(\tilde{W}^T S(z) - \epsilon\right). \quad (76)
$$

Theorem 2: Consider the following weight adaptation law for HONN employed in (74)

$$
\dot{\hat{W}} = \Gamma_W S\tilde{\varphi}^T P_W[0, \quad 1]^T - \sigma\Gamma_W\hat{W} \quad (77)
$$

where Γ_W and σ are suitably chosen positive definite matrix and positive scalar. Then, the tracking errors $\tilde{\varphi}_1$ and $\tilde{\varphi}_2$ in (76) will be eventually bounded into a small neighborhood around zero.

Proof: Let us rewrite the error dynamics (76) as

$$
\dot{\tilde{\varphi}} = A_m\tilde{\varphi} + b(v')[0, \quad 1]^T\left(\tilde{W}^T S(z) - \epsilon\right) \quad (78)
$$

where $A_m = \begin{bmatrix} 0 & 1 \\ -k_1 & -k_2 \end{bmatrix}$ satisfies the Lyapunov equation

$$
A_m^T P_W + P_W A_m = -Q_W \quad (79)
$$

i.e., for any symmetric positive definite matrix Q_W, there exists a symmetric positive definite P_W satisfying the aforementioned equation.

Considering the following Lyapunov function:

$$V_2(t) = \tilde{\varphi}^{\mathrm{T}} P_W \tilde{\varphi} + |b(v')| \tilde{W}^{\mathrm{T}} \Gamma_W^{-1} \tilde{W} \tag{80}$$

and the closed-loop dynamics (78) with the update law (77) and noticing that $b(v') < 0$, we obtain

$$
\begin{aligned}
\dot{V}_2(t) =& 2\tilde{\varphi}^{\mathrm{T}} P_W \dot{\tilde{\varphi}} + 2|b(v')| \tilde{W}^{\mathrm{T}} \Gamma_W^{-1} \dot{\tilde{W}} \\
=& 2\tilde{\varphi}^{\mathrm{T}} P_W A_m \tilde{\varphi} + 2\tilde{\varphi}^{\mathrm{T}} P_W b(v')[0, \quad 1]^{\mathrm{T}} \left(\tilde{W}^{\mathrm{T}} S(z) - \epsilon \right) \\
& + 2|b(v')| \tilde{W}^{\mathrm{T}} \Gamma_W^{-1} \Gamma_W S \tilde{\varphi}^{\mathrm{T}} P[0, \quad 1]^{\mathrm{T}} \\
& - 2|b(v')| \tilde{W}^{\mathrm{T}} \Gamma_W^{-1} \Gamma_W \sigma \hat{W} \\
=& \tilde{\varphi}^{\mathrm{T}} \left(A_m^{\mathrm{T}} P_W + P_W A_m \right) \tilde{\varphi} + 2|b(v')| \tilde{\varphi}^{\mathrm{T}} P_W [0, \quad 1]^{\mathrm{T}} \epsilon \\
& - 2\sigma |b(v')| \tilde{W}^{\mathrm{T}} (\tilde{W} + W^*) \\
\leq& - \tilde{\varphi}^{\mathrm{T}} Q_W \tilde{\varphi} - 2\sigma |b(v')| \|\tilde{W}\|^2 - 2\sigma |b(v')| \tilde{W}^{\mathrm{T}} W^* \\
& + 2|b(v')| \|\tilde{\varphi}^{\mathrm{T}} P_W [0, \quad 1]^{\mathrm{T}} \| \epsilon_0 \\
\leq& - \lambda_{Q_W} \|\tilde{\varphi}\|^2 - 2\sigma |b(v')| \|\tilde{W}\|^2 + \varepsilon^2 \|\tilde{\varphi}\|^2 + \varepsilon^2 \|\tilde{W}\|^2 \\
& + \frac{1}{\varepsilon^2} \epsilon_0^2 |b(v')|^2 \left\| P_W [0, \quad 1]^{\mathrm{T}} \right\|^2 \\
& + \frac{1}{\varepsilon^2} \sigma^2 |b(v')|^2 \|W^*\|^2 \tag{81}
\end{aligned}
$$

where $|\epsilon| \leq \epsilon_0$, λ_{Q_W} is the minimum eigenvalue of Q_W, and ε is any given positive constant which we can choose to be sufficiently small. Furthermore, we can choose the suitable Q_W and σ making $\lambda_{Q_W} \geq \varepsilon^2$ and $\sigma |b(v')| \geq \varepsilon^2$, and it follows that $\dot{V}_2(t) \leq 0$ in the complementary set of a set S_b defined as

$$S_b := \left\{ (\tilde{\varphi}, \tilde{W}) \left| \frac{\|\tilde{W}\|^2}{\bar{a}^2} + \frac{\|\tilde{\varphi}\|^2}{\bar{b}^2} - 1 \leq 0 \right. \right\} \tag{82}$$

with

$$\bar{a} = \frac{\frac{1}{\varepsilon} |b(v')| \sqrt{\epsilon_0^2 \|P_W [0, \quad 1]^{\mathrm{T}}\|^2 + \sigma^2 \|W^*\|^2}}{\sqrt{\lambda_{Q_W} - \varepsilon^2}}$$

$$\bar{b} = \frac{\frac{1}{\varepsilon} |b(v')| \sqrt{\epsilon_0^2 \|P_W [0, \quad 1]^{\mathrm{T}}\|^2 + \sigma^2 \|W^*\|^2}}{\sqrt{2\sigma |b(v')| - \varepsilon^2}}.$$

Obviously, the set S_b defined previously is compact. Hence, by LaSalle's theorem, it follows that all the solutions of (78) are bounded. The set S_b is shown in Fig. 3 and consists of the closed region bounded by the closed oval arc defined by $(\|\tilde{W}\|^2/\bar{a}^2) + (\|\tilde{\varphi}\|^2/\bar{b}^2) = 1$. Thus, the proof is completed. ■
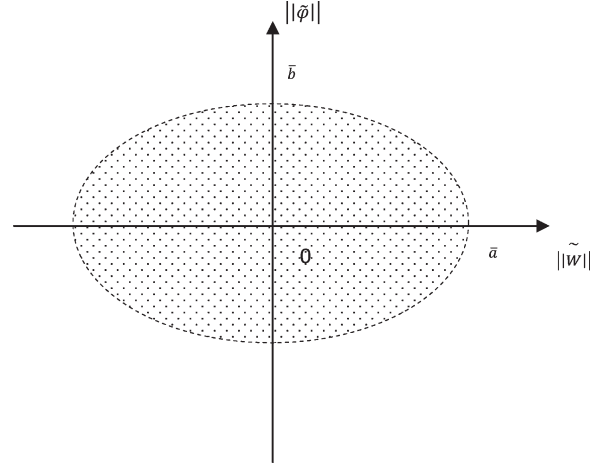

Fig. 3.   Bounding set of $\tilde{W}$ and $\|\tilde{\varphi}\|$.

VI. SIMULATION STUDIES

The overall control system scheme combining both adaptive controller and NN-based AGICT is shown in Fig. 4. The simulation study is carried out to verify the efficiency of both the controller and the trajectory generator. In the simulation study, the parameters of the WIP system (as shown in Fig. 1) are specified as follows: $M = 15.0$ kg, $I_w = 1.0$ kg · m², $I_M = 20$ kg · m², $m = 2.0$ kg, $L = 1$ m, $d = 1.0$ m, and $R = 0.5$ m. The simulation is carried out in 5 s, and the horizon t_f for LQR performance index is chosen as 3 s. The disturbances from environments on the system are introduced as $d_\alpha = 0.5 \sin(t)$ and $d_v = [0.3 \cos(2t), 0.3 \sin(t/2), 0.3 \sin(t)]$ in the simulation model. The desired trajectory for yaw angle is $\zeta_{1d} = -0.05t$ rad, and the initial yaw angle is set as $\zeta_1 = -3$ rad; the desired forward velocity is set as $\zeta_{2d} = 0$ while the initial velocity is 0.084 m/s. The design parameters of the LQR optimization performance index are $Q = \mathrm{diag}[5, 10]$ and $M_d = \mathrm{diag}[15, 15]$. The initial value of $\hat{\Theta}$ is $\hat{\Theta} = [0.27, 0.28, 0.16, 0.25]$, and the tuning gain matrix $\Gamma_\Theta = \mathrm{diag}[2, 2]$. The control gain matrix $K = \mathrm{diag}[40, 50]$. The HONN is constructed with $l = 65$ neurons, and for the initial weight estimate $\hat{W} \in R^l$, each element is selected as a random variable with a magnitude of 0.05. The tuning gain matrix and the forgetting factor of NN weight estimator are chosen as $\Gamma_W = \mathrm{diag}[0.5, 1]$ and $\sigma = 0.05$, respectively.

To demonstrate the efficiency of the proposed controller, we compare it with the model-based controller under the same operation condition and using the same NN reference trajectory generator for ξ_{3d}. The model-based controller is presented as $\tau_1 = D_{11}\ddot{\zeta}_{1d} + C_{11}\dot{\zeta}_1 + C_{13}\dot{\zeta}_3 - k_{11}(\dot{\zeta}_1 - \dot{\zeta}_{1d}) - k_{12}(\zeta_1 - \zeta_{1d})$ and $\tau_2 = -((D_{22}D_{33} - D_{23}^2(\zeta_3))/d_{23})\ddot{\zeta}_{3d} - k_{31}(\dot{\zeta}_3 - \dot{\zeta}_{3d}) - k_{32}(\zeta_3 - \zeta_{3d}) - C_{23}\dot{\zeta}_3 + (D_{22}/d_{23})(C_{31}\dot{\zeta}_1 + f_3 + g_3 + d_3) - (f_2 + g_2 + d_2))$ with $k_{11} = k_{12} = k_{31} = k_{32} = 12.0$, and it is assumed that there is 10% model uncertainty.

The tracking performance of the desired yaw angle is shown in Fig. 5, from which we see that, although the proposed controller response is less quicker, the controlled yaw trajectory exactly tracks the desired trajectory and there is no steady-state error, while the model-based controller could only track
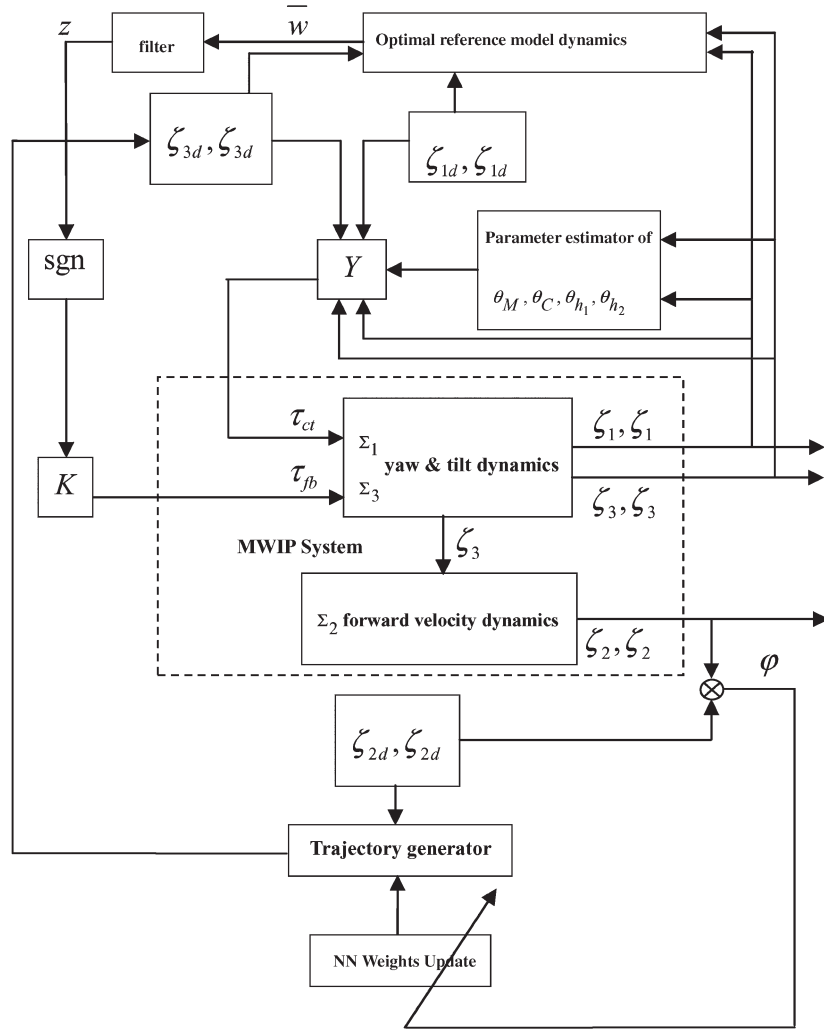
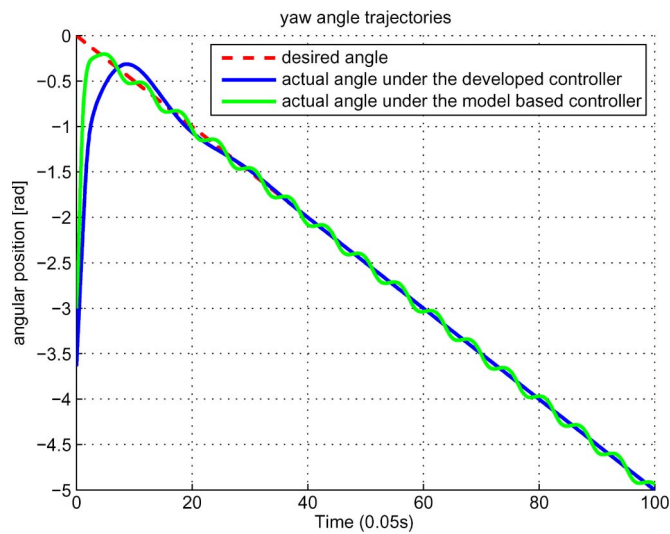Fig. 4. Scheme of overall system: Controller and trajectory generator.

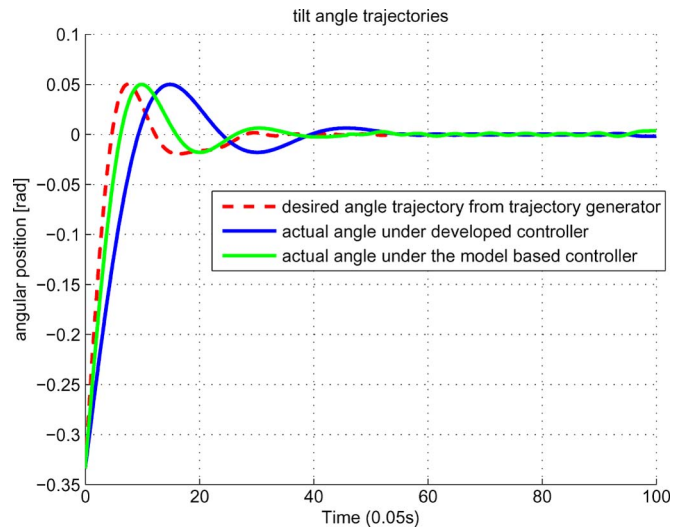Fig. 5. Comparison for the WIP yaw angle trajectories.

Fig. 6. Comparison for the WIP tilt angle trajectories.

the controlled yaw trajectory oscillating around the desired trajectory. The slightly slower response is due to the learning process of the adaptive controller, e.g., the estimated parameters need enough time to be adapted to suitable values. The tilt angle

trajectories are shown in Fig. 6, which shows that the reference trajectory of the tilt angle generated by the HONN will eventually be around zero in order to maintain the forward velocity at zero. Similar to the response of the yaw angle, the proposed
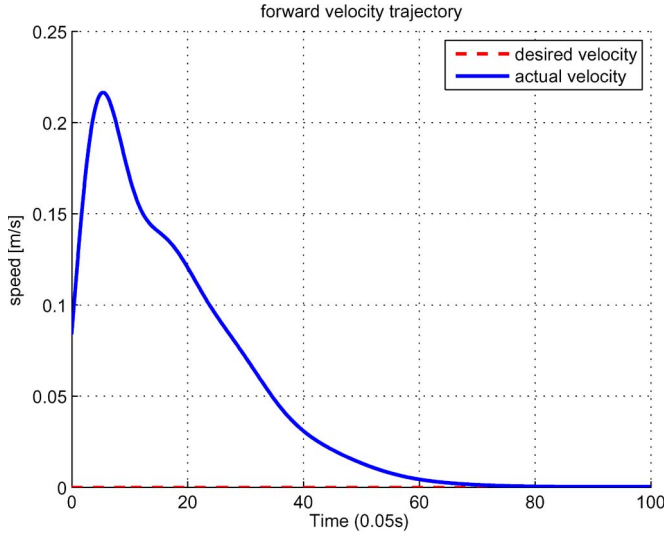
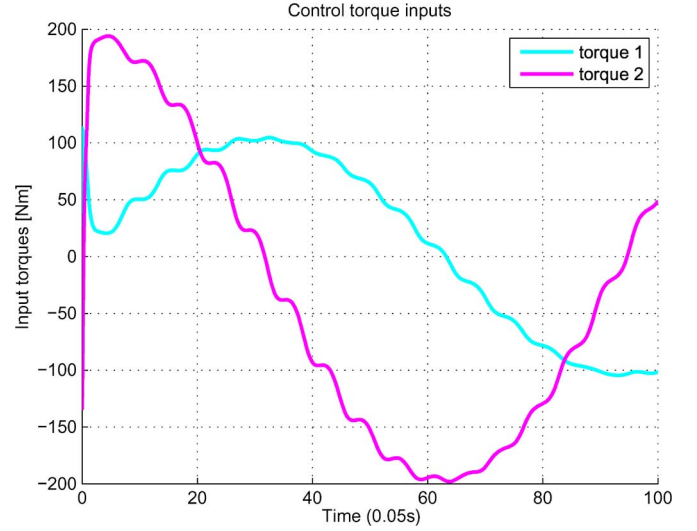Fig. 7. Trajectories of forward velocity.
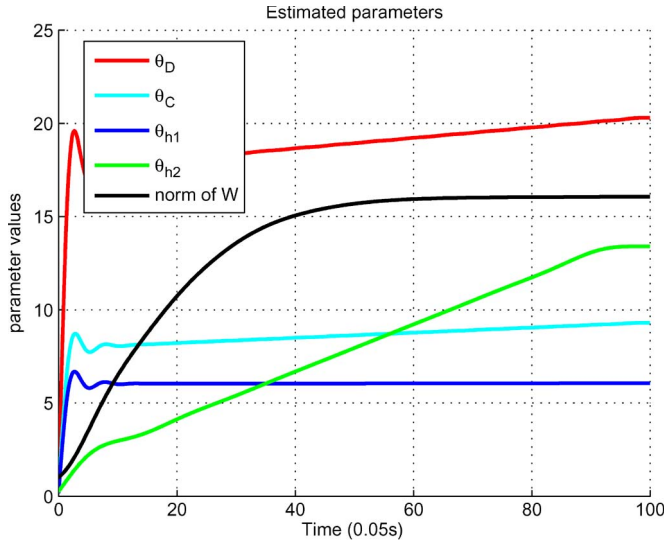

Fig. 9. Control torque inputs.

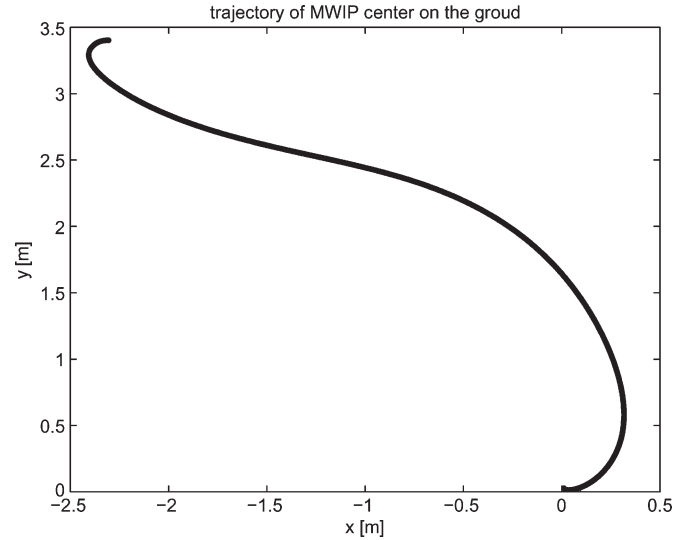Fig. 8. Control parameter estimation.

Fig. 10. Trajectory of WIP center projected unto the ground.

controller response is a little bit slower, but exact tracking is guaranteed. Fig. 7 shows that, under the effect of the reference tilt angle, the forward velocity will eventually converge to zero as we desire. The convergence of the forward velocity is slower than the convergence of tilt and yaw angles because, in addition to the adaptive controller parameter estimator adaptation, there is also the HONN weight adaptation. The boundedness of both controller parameter adaptation and HONN weight adaptation is shown in Fig. 8. The control torque inputs τ_1 and τ_2 are shown in Fig. 9, and the ground floor trajectory of the center of WIP is shown in Fig. 10.

As clearly shown by the simulation results, in the presence of totally unknown system parameters and external disturbance, the proposed adaptive variable structure controller is able to guarantee exact tracking of the tilt and yaw subsystem, while the HONN-generated tilt angle reference trajectory is able to maintain the forward velocity at the desired level. Therefore, the proposed controller is efficient in the presence of unknown non-

linear dynamic systems and environments. On the other hand, the model-based approach is sensitive to the accuracy of the dynamic model, as shown in Figs. 5 and 6, and more than 10% model parameter uncertainty will tend to make the closed-loop system unstable. In contrast, our proposed adaptive controller is able to tolerate complete unknown parameter uncertainty. This is one of the key advantages over the model-based controller. The controlled conditions in the test facility under which the parameters are identified are often very different from actual conditions, thus rendering the parameter inaccuracy for real operating conditions. In addition, the controlled closed-loop dynamics of the yaw and tilt subsystem are shaped through the LQR technique such that the optimization in terms of the performance index is achieved. It is also worth to mention that, in the "learning" mechanism of both the adaptive controller parameter and the HONN weight adaptation, once the estimates converge, they do not need to be "relearned" as long as there are significant changes of system dynamics and external conditions.

VII. Conclusion

In this paper, adaptive model reference control and NN-based trajectory planner have been designed on WIP systems for dynamic balance and motion tracking of desired trajectories. The dynamics of the subsystem consisting of the pendulum tilt angle and the mobile platform yaw angle has been shaped to follow a reference model, which is derived by using the LQR optimization technique to minimize both the motion tracking error and the transient acceleration for the best driving comfort. The forward velocity of the unactuated subsystem is made to track the desired motion by suitably designing a reference trajectory for the tilt angle, which directly affects the forward velocity. The proposed control method considers the presence of various uncertainties, including both parametric and functional uncertainties. The simulation results have demonstrated the efficiency of the proposed method.

References

[1] L. Wang, "Stable adaptive fuzzy controllers with application to inverted pendulum tracking," *IEEE Trans. Syst., Man, Cybern. B, Cybern.*, vol. 26, no. 5, pp. 677–691, Oct. 1996.

[2] R. Fierro, F. Lewis, and A. Lowe, "Hybrid control for a class of under-actuated mechanical systems," *IEEE Trans. Syst., Man, Cybern. A, Syst., Humans*, vol. 29, no. 6, pp. 649–654, Nov. 1999.

[3] W. S. Lu and Q. H. Meng, "Impedance control with adaptation for robotic manipulator," *IEEE Trans. Robot. Autom.*, vol. 7, no. 3, pp. 408–415, Jun. 1991.

[4] W. Chen and J. Li, "Decentralized output-feedback neural control for systems with unknown interconnections," *IEEE Trans. Syst., Man, Cybern. B, Cybern.*, vol. 38, no. 1, pp. 258–266, Feb. 2008.

[5] W. Chen, L. C. Jiao, and Z. B. Du, "Output-feedback adaptive dynamic surface control of stochastic nonlinear systems using neural network," *IET Control Theory Appl.*, vol. 4, no. 12, pp. 3012–3021, Dec. 2010.

[6] W. Chen, "Adaptive backstepping dynamic surface control for systems with periodic disturbances using neural networks," *IET Control Theory Appl.*, vol. 3, no. 10, pp. 1383–1394, Oct. 2009.

[7] W. Chen and Z. Zhang, "Globally stable adaptive backstepping fuzzy control for output-feedback systems with unknown high-frequency gain sign," *Fuzzy Sets Syst.*, vol. 161, no. 6, pp. 821–836, Mar. 2010.

[8] W. Chen, L. Jiao, J. Li, and R. Li, "Adaptive NN backstepping output-feedback control for stochastic nonlinear strict-feedback systems with time-varying delays," *IEEE Trans. Syst., Man, Cybern. B, Cybern.*, vol. 40, no. 3, pp. 939–950, Jun. 2010.

[9] M. Chen and S. S. Ge, "Robust adaptive neural network control for a class of uncertain MIMO nonlinear systems with input nonlinearities," *IEEE Trans. Neural Netw.*, vol. 21, no. 5, pp. 796–812, May 2010.

[10] M. Chen and S. S. Ge, "Adaptive tracking control of uncertain MIMO nonlinear systems with input saturation," *Automatica*, vol. 47, no. 3, pp. 452–465, Mar. 2011.

[11] S. Yang and M. Meng, "Neural network approaches to dynamic collision-free trajectory generation," *IEEE Trans. Syst., Man, Cybern. B, Cybern.*, vol. 31, no. 3, pp. 302–318, Jun. 2001.

[12] D. Xu, D. Zhao, J. Yi, and X. Tan, "Trajectory tracking control of omni-directional wheeled mobile manipulators: Robust neural network-based sliding mode approach," *IEEE Trans. Syst., Man, Cybern. B, Cybern.*, vol. 39, no. 3, pp. 788–799, Jun. 2009.

[13] W. Chen and L. Jiao, "Adaptive tracking for periodically time-varying and nonlinearly parameterized systems using multilayer neural networks," *IEEE Trans. Neural Netw.*, vol. 21, no. 2, pp. 345–351, Feb. 2010.

[14] V. Cherkassky, D. Ghering, and F. Mulier, "Comparison of adaptive methods for function estimation from samples," *IEEE Trans. Neural Netw.*, vol. 7, no. 4, pp. 969–984, Jul. 1996.

[15] E. B. Kosmatopoulos, M. M. Polycarpou, M. A. Christodoulou, and P. A. Ioannou, "High-order neural network structures for identification of dynamical systems," *IEEE Trans. Neural Netw.*, vol. 6, no. 2, pp. 422–431, Mar. 1995.

[16] P. Paretto and J. J. Niez, "Long term memory storage capacity of multi-connected neural networks," *Biol. Cybern.*, vol. 54, no. 1, pp. 53–63, 1986.

[17] C. L. Giles and T. Maxwell, "Learning, invariance, and generalization in high-order neural networks," *Appl. Opt.*, vol. 26, no. 23, pp. 4972–4978, Dec. 1987.

[18] M. M. Gupta and D. H. Rao, *Neuro-Control Systems: Theory and Applications*. New York: IEEE Press, 1994.

[19] M. M. Polycarpou and P. Ioannou, "Learning and convergence analysis of neural-type structured networks," *IEEE Trans. Neural Netw.*, vol. 3, no. 1, pp. 39–50, Jan. 1992.

[20] J. R. Munkres, *Analysis on Manifolds*. Reading, MA: Addison-Wesley, 1991.

[21] F. Grasser, A. Arrigo, S. Colombi, and A. C. Rufer, "JOE: A mobile, inverted pendulum," *IEEE Trans. Ind. Electron.*, vol. 49, no. 1, pp. 107–114, Feb. 2002.

[22] R. Brooks, L. Aryanada, A. Edsinger, P. Fitzpatrick, C. C. Kemp, U. O'Reilly, E. Torres-Jara, P. Varshavskaya, and J. Weber, "Sensing and manipulating built-for-human environments," *Int. J. Humanoid Robot.*, vol. 1, no. 1, pp. 1–28, Mar. 2004.

[23] Z. Li and J. Luo, "Adaptive robust dynamic balance and motion controls of mobile wheeled inverted pendulums," *IEEE Trans. Control Syst. Technol.*, vol. 17, no. 1, pp. 233–241, Jan. 2009.

[24] K. Pathak, J. Franch, and S. K. Agrawal, "Velocity and position control of a wheeled inverted pendulum by partial feedback linearization," *IEEE Trans. Robot.*, vol. 21, no. 3, pp. 505–513, Jun. 2005.

[25] N. R. Gans and S. A. Hutchinson, "Visual servo velocity and pose control of a wheeled inverted pendulum through partial-feedback linearization," in *Proc. IEEE/RSJ Int. Conf. Intel. Robots Syst.*, 2006, pp. 3823–3828.

[26] G. Campion, G. Bastin, and B. Dandrea-Novel, "Structural properties and classification of kinematic and dynamic models of wheeled mobile robots," *IEEE Trans. Robot. Autom.*, vol. 12, no. 1, pp. 47–62, Feb. 1996.

[27] Z. Li, C. Yang, and J. Gu, "Neuro-adaptive compliant force/motion control for uncertain constrained wheeled mobile manipulator," *Int. J. Robot. Autom.*, vol. 22, no. 3, pp. 206–214, 2007.

[28] H. Arai and K. Tanie, "Nonholonomic control of a three-DOF planar underactuated manipulator," *IEEE Trans. Robot. Autom.*, vol. 14, no. 5, pp. 681–694, Oct. 1998.

[29] A. De Luca and G. Oriolo, "Trajectory planning and control for planar robots with passive last joint," *Int. J. Robot. Res.*, vol. 21, no. 5–6, pp. 575–590, May 2002.

[30] Z. Li and C. Yang, "Neural-adaptive output feedback control of a class of transportation vehicles based on wheeled inverted pendulum models," *IEEE Trans. Control Syst. Technol.*, 2011. doi:10.1109/ TCST.2011.216822, to be published.

[31] Z. Li and Y. Zhang, "Robust adaptive motion/force control for wheeled inverted pendulums," *Automatica*, vol. 46, no. 8, pp. 1346–1353, Aug. 2010.

[32] W. S. Lu and Q. H. Meng, "Impedance control with adaptation for robotic manipulations," *IEEE Trans. Robot. Autom.*, vol. 7, no. 3, pp. 408–415, Jun. 1991.

[33] R. Colbaugh, H. Seraji, and K. Glass, "Direct adaptive impedance control of manipulators," in *Proc. 30th Conf. Decision Control*, 1991, pp. 2410–2415.

[34] K. Wedeward and R. Colbaugh, "New stability results for direct adaptive impedance control," in *Proc. IEEE Int. Symp. Intell. Control*, 1995, pp. 281–287.

[35] A. R. Barron, "Universal approximation bounds for superposition for a sigmoidal function," *IEEE Trans. Inf. Theory*, vol. 39, no. 3, pp. 930–945, May 1993.

[36] T. P. Chen and H. Chen, "Approximation capability to functions of several variables, nonlinear functionals, and operators by radial basis function neural networks," *IEEE Trans. Neural Netw.*, vol. 6, no. 4, pp. 904–910, Jul. 1995.

[37] V. Cherkassky, D. Ghering, and F. Mulier, "Comparison of adaptive methods for function estimation from samples," *IEEE Trans. Neural Netw.*, vol. 7, no. 4, pp. 969–984, Jul. 1996.

[38] E. B. Kosmatopoulos, M. M. Polycarpou, M. A. Christodoulou, and P. A. Ioannou, "High-order neural network structures for identification of dynamical systems," *IEEE Trans. Neural Netw.*, vol. 6, no. 2, pp. 422–431, Mar. 1995.

[39] P. Paretto and J. J. Niez, "Long term memory storage capacity of multiconnected neural networks," *Biol. Cybern.*, vol. 54, no. 1, pp. 53–63, May 1986.

[40] C. L. Giles and T. Maxwell, "Learning, invariance, and generalization in high-order neural networks," *Appl. Opt.*, vol. 26, no. 23, pp. 4972–4978, Dec. 1987.

[41] M. M. Gupta and D. H. Rao, *Neuro-Control Systems: Theory and Applications*. New York: IEEE Press, 1994.

[42] M. M. Polycarpou and P. Ioannou, "Learning and convergence analysis of neural-type structured networks," *IEEE Trans. Neural Netw.*, vol. 3, no. 1, pp. 39–50, Jan. 1992.

[43] J. R. Munkres, *Analysis on Manifolds*. Reading, MA: Addison-Wesley, 1991.

[44] B. D. O. Anderson and J. B. Moore, *Optimal Control*. London, U.K.: Prentice-Hall, 1989.

[45] B. Siciliano, L. Sciavicco, L. Villani, and G. Oriolo, *Robotics: Modelling, Planning and Control*. New York: Springer-Verlag, 2008.

[46] H. K. Khalil, *Nonlinear Systems*., 3rd ed. Upper Saddle River, NJ: Prentice-Hall, 2002.

[47] Y. J. Liu, C. L. P. Chen, G. X. Wen, and S. C. Tong, "Adaptive neural output feedback tracking control for a class of uncertain discrete-time nonlinear systems," *IEEE Trans. Neural Netw.*, vol. 22, no. 7, pp. 1162–167, Jul. 2011.

[48] W. Chen, L. Jiao, R. Li, and J. Li, "Adaptive backstepping fuzzy control for nonlinearly parameterized systems with periodic disturbances," *IEEE Trans. Fuzzy Syst.*, vol. 18, no. 4, pp. 674–685, Aug. 2010.

[49] R. Cui and W. Yan, "Mutual synchronization of multiple robot manipulators with unknown dynamics," *J. Intell. Robot. Syst.*, Apr. 2012. doi:10.1007/s10846-012-9674-9, to be published.

[50] Y. J. Liu, S. C. Tong, D. Wang, T. S. Li, and C. L. P. Chen, "Adaptive neural output feedback controller design with reduced-order observer for a class of uncertain nonlinear SISO systems," *IEEE Trans. Neural Netw.*, vol. 22, no. 8, pp. 1328–1334, Aug. 2011.

[51] R. Cui, W. Yan, and D. Xu, "Synchronization of multiple autonomous underwater vehicles without velocity measurements," *Sci. China Inf. Sci.*, 2012. doi:10.1007/s11432-012-4579-6, to be published.

[52] Y. J. Liu and W. Wang, "Adaptive fuzzy control for a class of uncertain nonaffine nonlinear systems," *Inf. Sci.*, vol. 177, no. 18, pp. 3901–3917, Sep. 2007.

[53] Y. J. Liu, W. Wang, S. C. Tong, and Y. S. Liu, "Robust adaptive tracking control for nonlinear systems based on bounds of fuzzy approximation parameters," *IEEE Trans. Syst., Man, Cybern. A, Syst., Humans*, vol. 40, no. 1, pp. 170–184, Jan. 2010.

[54] R. Cui, B Gao, and J. Guo, "Pareto-optimal coordination of multiple robots with safety guarantees," *Autonomous Robots*, vol. 32, no. 3, pp. 189–205, 2012.

[55] C. Yang, S. S. Ge, C. Xiang, T. Chai, and T. H. Lee, "Output feedback NN control for two classes of discrete-time systems with unknown control directions in a unified approach," *IEEE Trans. Neural Netw.*, vol. 19, no. 11, pp. 1873–1886, Nov. 2008.
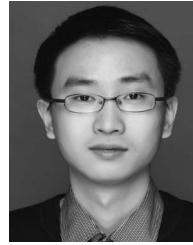
Chenguang Yang (M'10) received the B.Eng. degree in measurement and control from Northwestern Polytechnical University, Xi'an, China, in 2005 and the Ph.D. degree in control engineering from the National University of Singapore, Singapore, in 2010.

From October 2009 to December 2010, he was a Research Associate with Imperial College London, London, U.K., working on human–robot interaction. Since December 2010, he has been a Lecturer of robotics with the School of Computing and Mathematics, Plymouth University, Plymouth, U.K., where he is currently on secondment as a Marie Curie International Incoming Fellow from August 2011, supported by the European Commission. His current research interests include robotics, control, and human–robot interaction.

Zhijun Li (M'07–SM'09) received the Dr.Eng. degree in mechatronics from Shanghai Jiao Tong University, Shanghai, China, in 2002.

From 2007 to 2011, he was an Associate Professor with the Department of Automation, Shanghai Jiao Tong University. He is currently a Professor with the College of Automation, South China University of Technology, Guangzhou, China. His current research interests include adaptive/robust control, mobile manipulator, teleoperation system, etc.
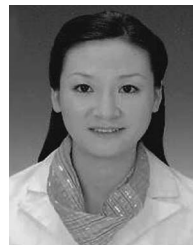
Jing Li received the Ph.D degree in applied mathematics from Xidian University. Xi'an, China, in 2010.

From September 2009 to July 2010, she was a Visiting Scholar with the School of Control Science and Engineering, Shandong University, Jinan, China. From October 2011 to April 2012, she was an Academic Visitor in robotics with Plymouth University, Plymouth, U.K. Since April 2012, she has been a Visiting Researcher in human–robot interaction with Imperial College London, London, U.K. She is also currently an Associate Professor with Xidian University. Her current research interests include adaptive neural network control, stochastic control, robotics, and human–robot interaction.